Modelling of Magnetic Anisotropy in Electrical Steel Sheet by Means of Cumulative Distribution Functions of Gaussians

Guilherme Costa Ayres Tolentino, Jean Leite, Mathieu Rossi, Olivier Ninet, Guillaume Parent, Jonathan Blaszkowski

Modelling of magnetic anisotropy in electrical steel sheet by means of cumulative distribution functions of Gaussians

Guilherme C. A. Tolentino[1], Jean V. Leite[2], Mathieu Rossi[1], Olivier Ninet[1], Guillaume Parent[1] and Jonathan Blaszkowski[3]
[1]Univ. Artois, UR 4025, Laboratoire Systèmes Électrotechniques et Environnement (LSEE), F-62400 Béthune, France
[2]Universidade Federal de Santa Catarina, GRUCAD, Santa Catarina, Florianòpolis, Brazil
[3]Thyssenkrupp Electrical Steel, F-62330 Isbergues, France

This paper proposes a methodology for modeling magnetic anisotropy in ferromagnetic materials. This approach was initially used to represent the isothermal remanent magnetization (IRM) acquired by natural mineral assemblages and based on the use of the cumulative distribution function (CDF) of a probability density function (PDF). For the purpose of this work, the anisotropy of electrical steel sheets is modeled by means of cumulative distribution functions of Gaussians. The methodology is validated by comparisons between numerical and experimental data obtained from an Epstein frame and a Rotational Single Sheet Tester. The outcomes of the study are twofold: firstly, the parameters defining the CDF follow a polynomial trendline and secondly, they can easily be calculated from a limited amount of experimental data which is a key point from an engineering point of view.

***Index Terms*—Magnetic anisotropy, non oriented electrical steel, grain oriented electrical steel, first magnetization curves modeling, cumulative distribution functions.**

I. Introduction

DEVELOPING a model of magnetic materials, such as electrical steel, that allows to account for both their nonlinear and anisotropic behavior remains a challenge. In the past decades, several approaches aiming to achieve this goal have been presented, each with their particular strengths and weaknesses. In the earliest approach the magnetic induction $\mathbf{B}$ is related to the magnetic field $\mathbf{H}$ by means of a diagonal tensor composed of magnetic permeabilities along the Rolling Direction (RD), the Transverse Direction (TD) and the Orthogonal Direction (OD) [1]. The main drawback of this method lies in the fact that the relationship between $\mathbf{B}$ and $\mathbf{H}$ along any other direction than the RD, TD and OD are naturally obtained through linear interpolations, making both its accuracy and relevance questionable. This point has been slightly improved with the elliptical model [2] by using nonlinear interpolations. Nevertheless, both methods remain not representative enough of the actual anisotropic behavior of electrical steel. In order to solve this difficulty, another approach based on the use of a set of first magnetization curves along several magnetization directions is proposed in [3] and [4]. Nevertheless, this approach requires a very large amount of experimental data which is a major drawback from an engineering point of view. According to [5,6] , the approach based on the orientation distribution theory [7] allows to establish a model accounting for any magnetization direction while requiring a limited amount of experimental data. Nevertheless, as pointed out in [8] it involves the computation of numerous nonlinear coefficients and the amount of required experimental data remains significant.

The approach followed in this paper is based on the one introduced by Roberston and France [9] who noticed that the shape of an isothermal remanent magnetization (IRM) acquisition curves of a natural mineral assemblage is very similar to the one of a cumulative log Gaussian. It can be noted that Paesano *et al.* also noticed the similarity between another type of CDF, that is the complementary of the Hill equation, in [10].The aim of the work presented in this paper is to enhance the approach based on Gaussian CDF in order to establish a mathematical expression of the constitutive relation between $\mathbf{B}$ and $\mathbf{H}$ that accounts for both the nonlinear and anisotropic behavior of electrical steel while keeping the number of experimental data as low as possible. The key outlines of the presented study are multiple. Firstly, to the authors' knowledge, this approach has never been used in the case of first magnetization curve of electrical steel modeling although it has been used to deal with a statistical approach of hysteresis phenomenon [11]. Secondly it is highlighted that the nonlinear behavior of electrical steel can be accurately taken into account by using the cumulative distribution function (CDF) of a sum of probability density functions (PDF) instead of just one PDF. Thirdly, it is shown that the anisotropic behavior of electrical steel can be taken into account by defining θ-dependant PDFs, where θ is the angle between $\mathbf{H}$ and the RD of the steel sheet. Fourthly, it is shown that those parameters defining the PDF are easy to calculate from a very limited amount of experimental data.

The paper is structured as follows. In Section II the theoretical framework is presented. In particular, the way a CDF can be shaped in order to match a first magnetization curve is detailed. Moreover, θ-dependant parameters defining the CDF are introduced. In Section III the model is tested and validated on four different electrical steel grades. Section IV, as for it, is devoted to the exploitation of the model.

II. Theoretical Framework

A. PDF, CDF and first magnetization curve

Let a PDF parametrized in terms of the mean and the variance, denoted by μ and σ^2 respectively:

$$f(x) = \frac{1}{\sigma\sqrt{2\pi}}\, e^{-\frac{1}{2}\left(\frac{x-\mu}{\sigma}\right)^2}. \tag{1}$$

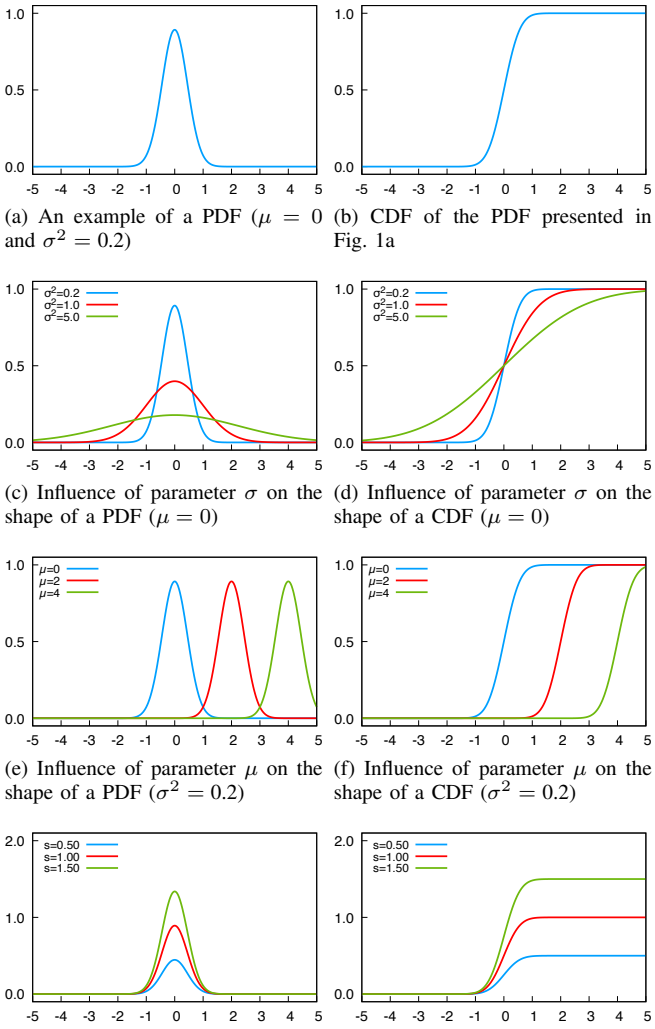

(a) An example of a PDF ($\mu = 0$ and $\sigma^2 = 0.2$)
(b) CDF of the PDF presented in Fig. 1a
(c) Influence of parameter σ on the shape of a PDF ($\mu = 0$)
(d) Influence of parameter σ on the shape of a CDF ($\mu = 0$)
(e) Influence of parameter μ on the shape of a PDF ($\sigma^2 = 0.2$)
(f) Influence of parameter μ on the shape of a CDF ($\sigma^2 = 0.2$)
(g) Influence of parameter s on the shape of a PDF ($\mu = 0$ and $\sigma^2 = 0.2$)
(h) Influence of parameter s on the shape of a CDF ($\mu = 0$ and $\sigma^2 = 0.2$)

Fig. 1. Influence of parameters σ, μ and s on the shape of a PDF and a CDF

The associated CDF, which is the area under the PDF curve from $-\infty$ to x, can be expressed in terms of the error function $\text{erf}(x) = \frac{2}{\sqrt{\pi}} \int_0^x e^{-t^2} \text{d}t$ [12], leading to:

$$F(x) = \int_{-\infty}^{x} f(z)\text{d}z = \frac{1}{2}\left[1 + \text{erf}\left(\frac{x-\mu}{\sigma\sqrt{2}}\right)\right]. \quad (2)$$

As an illustration $f(x)$ and $F(x)$ are presented in Figs. 1a and 1b respectively. One can notice the great similarity of the shape of the CDF and the one of a magnetization curve as originally pointed out by Roberston and France [9]. Therefore, it appears possible to shape a CDF by playing on the aformentioned parameters. Firstly, parameter σ allows to define the slope of the linear part of the CDF as shown in Figs. 1c and 1d. Then, parameter μ allows to shift the position of this linear part of the CDF along the abscissa axis. Finally, since $\lim_{x\to+\infty} \text{erf}(x) = 1$ a scaling factor, denoted s, is to be introduced in order to allow the maximum value of the CDF to be greater than 1 (Figs. 1g and 1h).

B. Modeling first magnetization curves of electrical steel by means of CDF

The first magnetization curve can be expressed either in terms of magnetic induction B or magnetization M. Since $\lim_{H\to+\infty} B(H) = \mu_0 H$ whereas $\lim_{x\to+\infty} \text{erf}(x) = 1$, relation (2) has to be used to model M. Then, B can be classically defined as $B(H) = \mu_0 (H + M)$. Nevertheless, (2) can not be used to express M as it is. As a matter of fact, $M(0) = 0$ whereas $F(x) > 0, \forall x \in \mathbb{R}$. To solve this problem, let us define a function $G(x)$ such that:

$$\begin{aligned} G(x) &= s\left(F(x) - F(0)\right) \\ &= s\left(\int_{-\infty}^{x} f(z)\text{d}z - \int_{-\infty}^{0} f(z)\text{d}z\right) \\ &= \frac{s}{2}\left[\text{erf}\left(\frac{x-\mu}{\sigma\sqrt{2}}\right) - \text{erf}\left(\frac{-\mu}{\sigma\sqrt{2}}\right)\right] \end{aligned} \quad (3)$$

which, once rewritten in terms of magnetization and magnetic field, leads to:

$$M(H) = \frac{s}{2}\left[\text{erf}\left(\frac{H-\mu}{\sigma\sqrt{2}}\right) - \text{erf}\left(\frac{-\mu}{\sigma\sqrt{2}}\right)\right] \quad (4)$$

Although Robertson and France proposed to use one CDF to model an IRM curve [9], Stockhausen [13] and Leonhardt [14] pointed out that using a sum of CDFs instead of just one leads to a better accuracy. Then, (4) becomes:

$$M(H) = \sum_{i=1}^{N} \frac{s_\text{i}}{2}\left[\text{erf}\left(\frac{H-\mu_\text{i}}{\sigma_\text{i}\sqrt{2}}\right) - \text{erf}\left(\frac{-\mu_\text{i}}{\sigma_\text{i}\sqrt{2}}\right)\right] \quad (5)$$

where N is the number of CDFs.

C. Taking anisotropy into account

As defined in Section II-B, the values of the three parameters σ, μ and s are scalars linked to the studied material. In this way, the model defined by (5) allows to deal with isotropic material only. We propose to enhance it by defining each of the three parameters σ, μ and s as functions of θ instead of scalars, where θ is the angle between $\mathbf{H}$ and the RD of the considered electrical steel sheet. Then, the constitutive relation that relates B and H and that allows to account for both the saturation and the anisotropy can be expressed as:

$$\begin{aligned} B(H,\theta) = \mu_0 \Bigg[& H + \\ & \sum_{i=1}^{N} \frac{s_i(\theta)}{2}\left[\text{erf}\left(\frac{H-\mu_i(\theta)}{\sigma_i(\theta)\sqrt{2}}\right) - \text{erf}\left(\frac{-\mu_i(\theta)}{\sigma_i(\theta)\sqrt{2}}\right)\right]\Bigg]. \end{aligned} \quad (6)$$

III. Identification of parameters and model validation

A. Tested electrical steel grades

In this Section, the proposed model governed by (6) is tested and validated on two different non oriented (NO) as well as two different grain oriented (GO) electrical steel grades denoted by M530-50A, M270-35A, M11535P and CGO35 respectively. It is worth pointing out that contrary to what

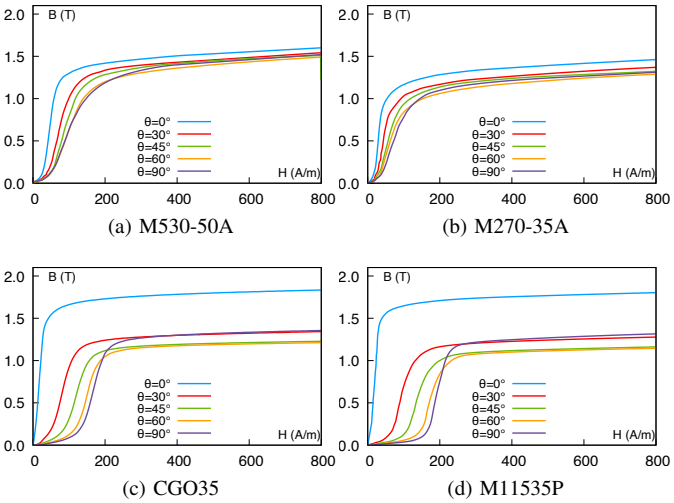

(a) M530-50A (b) M270-35A

(c) CGO35 (d) M11535P

Fig. 2. Experimental data for different electrical steels grades

their classification suggests the two NO grades present a non negligible anisotropic behavior which makes them worthwhile candidates to validate the proposed model. As an illustration, the first magnetization curves obtained experimentally for each of the four grades are presented in Fig. 2 for five different magnetization directions ($\theta = \{0°, 30°, 45°, 60°, 90°\}$). Two different magnetic characterization devices were used to obtain those curves. The NO samples (M530-50A and 270-35A) were characterized using a vertical rotating single sheet tester [15]. It is composed of two yokes – and therefore two phases – arranged along each side of the test sample, which is a square of 300 mm side length and one sheet thickness. As in the case of the horizontal single sheet tester, [16]this device allows to magnetize the sample along any direction, under pulsating or rotating conditions. In our case, the curves presented in Fig. 2 were obtained by applying a pulsating magnetization field along the aforementioned θ angle. The GO (M11535P and CGO35) were characterized using the standardized Epstein frame [17]. In this case, the samples, whose size are 300 mm × 30 mm are cut at different θ angles to the RD. In this way, each leg of the Epstein frame is magnetized along θ.

B. Influence of the number of CDF

As mentioned in [13,14] the number of CDFs used in (6) has an impact on the accuracy of the model. To evaluate this impact, parameters σ_i, μ_i and s_i are determined by fitting (6) to the experimental data of Fig. 2 for each grade, for each value of θ and for $N = \{1, 2, 3, 4\}$. Table I gathers all the maximum absolute errors, denoted by ΔB, obtained when comparing the first magnetization curves obtained by (6) to the experimental data. In the following the maximum absolute error is defined by $\Delta B(H) = \max\{|B_{\text{exp}}(H) - B_{\text{mod}}(H)| : H \in \mathbb{R}^+\}$ where $B_{\text{exp}}(H)$ and $B_{\text{mod}}(H)$ are the values of the magnetic induction obtained experimentally and (6) respectively.

The review of this Table indicates that:

1) $N = 1$ leads to the greatest gaps between the curves given by the model and the experimental data;

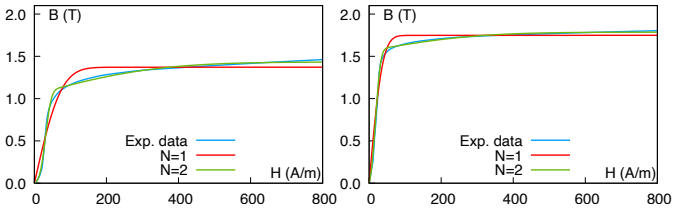

(a) M270-35A (b) M11535P

Fig. 3. Comparison between first magnetization obtained by means of (6) for $\theta = 0°$, $N = \{1, 2\}$ and experimental data.

2) using $N > 2$ does not improve substantially the accuracy of the model compared to $N = 2$.

As an illustration, Fig. 3 shows a comparison between the experimental data and the curves obtained from the model ($N = \{1, 2\}$) on the least favorable case reported in Table I, that is $\theta = 0°$, for both NO and GO grades.

In consequence, N is set to 2 for all results presented in the following.

C. Taking into account the anisoptropy: evolution of parameters σ, μ and s with θ

As mentioned in Section II, the aim of the presented work is to make (5) able to deal with anisotropic material by making each of the three parameters defining the CDFs θ-dependant. Hence, a particular focus is placed here on the analysis of the evolution of those parameters with θ in order to obtain trends. Fig. 4 shows the evolution of $\sigma_i(\theta)$, $\mu_i(\theta)$ and $s_i(\theta)$ with $i = \{1, 2\}$ for M530-50A and M11535P.

The analysis of the evolution of those three parameters for each tested grade leads to two key outcomes:

1) all the parameters follow a polynomial trendline whatever the grade;
2) the degree of each polynomial is equal to 2 (see Table II).

In order to validate those outcomes all the three parameters are now calculated by the polynomials of Table II and used in (6) to generate new first magnetization curves. The maximum absolute errors obtained when comparing those first magnetization curves to experimental data are gathered in Table III. It can be seen that those maximum absolute errors are in the same order of magnitude as those presented in Table I.

This validates that 2nd order polynomials can be used to determine all the parameters defining (6), which makes the model able to determine any first magnetization curve along any θ from a limited amount of experimental data. As a matter of fact, the number of required experimental data is equal to the order of the polynomial plus 1.

It may be noted that some of the terms of 2nd order of polynomials in Table II seem negligible. This is e.g. the case for polynomials governing σ_1 and μ_2. Nevertheless, as negligible they might seem, it turns out those terms have a significant influence on the final accuracy of the model. As an example, in the case of σ_1 the term of 2nd order can represent up to 26 % – for $\theta = 90°$ – of the total value of

TABLE I
MAXIMUM ABSOLUTE ERRORS BETWEEN FIRST MAGNETIZATION CURVES OBTAINED BY (6) AND EXPERIMENTAL DATA. ALL VALUES ARE IN mT

N	1					2					3					4				
θ	0°	30°	45°	60°	90°	0°	30°	45°	60°	90°	0°	30°	45°	60°	90°	0°	30°	45°	60°	90°
M530-35A	157	128	127	136	125	61	66	52	38	46	68	125	70	45	36	100	116	64	44	37
M270-35A	196	195	181	169	118	133	112	134	71	45	81	200	101	68	35	117	193	83	63	35
M11535P	254	107	127	147	180	116	75	69	62	65	131	58	57	55	52	70	45	57	49	55
CGO35	139	179	148	158	165	76	32	27	32	26	68	21	18	20	18	21	16	17	18	25

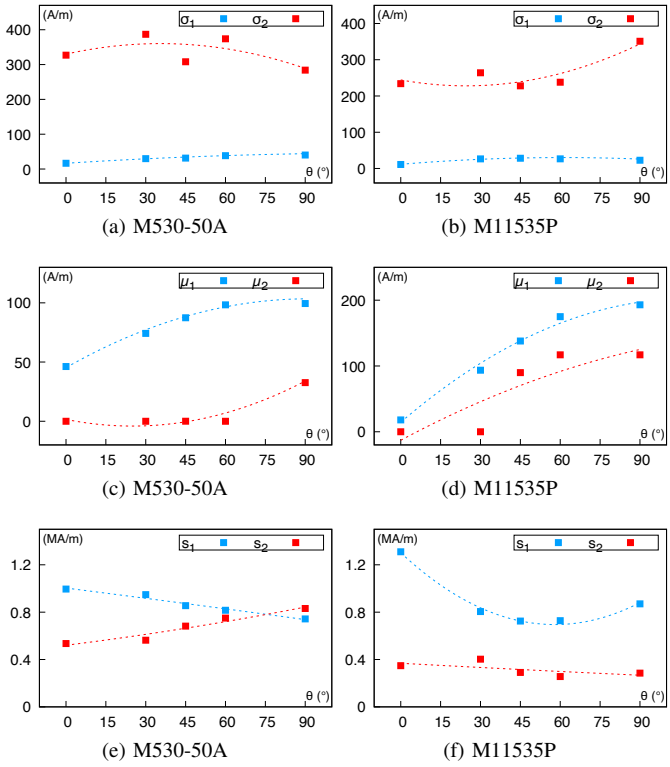

(a) M530-50A (b) M11535P (c) M530-50A (d) M11535P (e) M530-50A (f) M11535P

Fig. 4. Evolution of σ_i, μ_i and s_i with θ. Square marks and dashed lines represent experimental data and trend lines respectively.

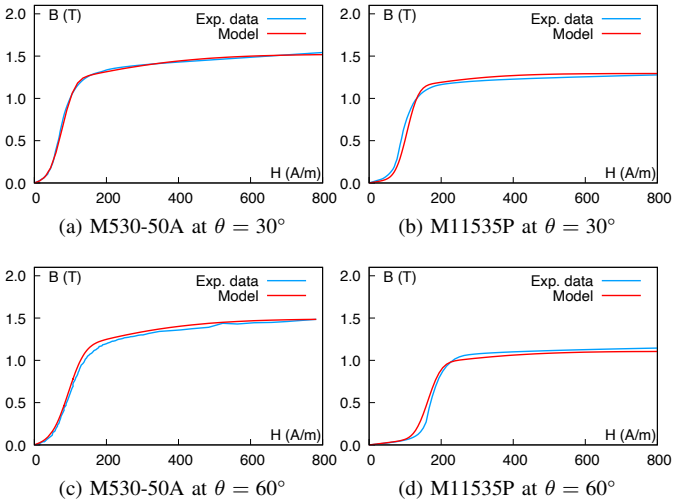

(a) M530-50A at $\theta = 30°$ (b) M11535P at $\theta = 30°$ (c) M530-50A at $\theta = 60°$ (d) M11535P at $\theta = 60°$

Fig. 5. Comparison between first magnetization obtained by means of (6) for $\theta = \{30°, 60°\}$. Parameters σ_i, μ_i and s_i are polynomials determined from three experimental data ($\theta = \{0°, 45°, 90°\}$) only.

the polynomial. Then, the absolute errors between the model and the experimental data is doubled for the GO grades when a 1st order polynomial is used for σ_1.

IV. MODEL EXPLOITATION: REDUCING THE AMOUNT OF REQUIRED EXPERIMENTAL DATA AND PREDICTING THE MAGNETIC BEHAVIOR AT ANY θ

Results presented in Section III highlighted that the three parameters used in (6) can be derived from 2nd order polynomials obtained from experimental data. Still in Section III, they are determined from five experimental data, which is obviously more than enough for such an order.

Here the 2nd order polynomials governing the evolution of parameters σ_i, μ_i and s_i with θ are determined from $\theta = \{0°, 45°, 90°\}$ only and used in (6) to generate new first magnetization curves again. Our aim here is twofold: to analyze the impact of using only three experimental data on the accuracy of the model and, more important, to generate first magnetization curves along magnetization directions that are not involved in the determination of parameters σ_i, μ_i and s_i, i.e. that are not involved in the determination of (6).

Table IV gathers all the maximum absolute errors obtained when comparing the first magnetization curves obtained by (6) in such conditions to the experimental data. The review of this Table indicates that:

1) for $\theta = \{0°, 45°, 90°\}$ the maximum absolute errors are almost identical to those reported in Table I, i.e. when the CDFs in (6) are directly determined by fitting to the experimental data. This was expected given the fact that the polynomial has been generated from those specific angles;
2) for 30° and 60° the maximum absolute errors are in the same order of magnitude as those reported in Table I.

The magnetization curves along $\theta = \{30°, 60°\}$ are presented in Fig. 5. One can notice the great concordance between the curves generated by the model and experimental data.

Those outcomes imply that the model governed by (6) can be fully determined with an amount of experimental data limited to three magnetization directions only, which is an important enhancement compared to others methods dealt in the literature [3]–[5,8].

TABLE II
POLYNOMIAL EXPRESSION OF $\sigma_i(\theta)$, $\mu_i(\theta)$ AND $s_i(\theta)$ OBTAINED FROM 5 EXPERIMENTAL DATA

	M530-50A	M270-35A	M11535P	CGO35
σ_1	$-0.002\,\theta^2 + 0.486\,\theta + 16.581$	$-0.001\,\theta^2 + 0.292\,\theta + 12.216$	$-0.005\,\theta^2 + 0.610\,\theta + 11.520$	$-0.004\,\theta^2 + 0.444\,\theta + 14.675$
σ_2	$-0.024\,\theta^2 + 1.705\,\theta + 329.956$	$-0.002\,\theta^2 + 0.767\,\theta + 268.711$	$0.027\,\theta^2 - 1.328\,\theta + 244.339$	$0.011\,\theta^2 - 0.479\,\theta + 238.923$
μ_1	$-0.007\,\theta^2 + 1.276\,\theta + 45.248$	$-0.002\,\theta^2 + 0.643\,\theta + 30.519$	$-0.016\,\theta^2 + 3.469\,\theta + 14.487$	$-0.013\,\theta^2 + 2.957\,\theta + 11.770$
μ_2	$0.009\,\theta^2 - 0.450\,\theta + 1.552$	$0.000\,\theta^2 + 0.000\,\theta + 0.000$	$-0.007\,\theta^2 + 2.164\,\theta - 12.934$	$0.001\,\theta^2 + 0.080\,\theta - 1.327$
s_1	$-1.160\,\theta^2 - 2859.113\,\theta + 1e06$	$33.200\,\theta^2 - 4377.696\,\theta + 8.5e5$	$180.685\,\theta^2 - 2.1e4\,\theta + 1.3e6$	$190.968\,\theta^2 - 2.4e6\,\theta + 1.4e6$
s_2	$8.585\,\theta^2 + 2811.496\,\theta + 5.2e5$	$-19.069\,\theta^2 + 2055.501\,\theta + 6e5$	$1.013\,\theta^2 - 1213.151\,\theta + 3.7e5$	$5.747\,\theta^2 + 53.779\,\theta + 3.9e5$

TABLE III
MAXIMUM ABSOLUTE ERRORS BETWEEN EXPERIMENTAL DATA AND FIRST MAGNETIZATION CURVES OBTAINED BY (6) WHEN σ_i, μ_i AND s_i ARE CALCULATED BY MEANS OF THE 2ND ORDER POLYNOMIAL PRESENTED IN TABLE II. ALL VALUES ARE IN mT

θ	0°	30°	45°	60°	90°
M530-50A	69	81	62	68	45
M270-35A	104	128	130	61	54
M11535P	199	179	38	179	67
CGO35	164	121	29	118	30

TABLE IV
MAXIMUM ABSOLUTE ERRORS BETWEEN EXPERIMENTAL DATA AND FIRST MAGNETIZATION CURVES OBTAINED BY (6) WHEN WHEN σ_i, μ_i AND s_i ARE CALCULATED BY MEANS OF THE 2ND ORDER POLYNOMIAL EVALUATED FROM 3 EXPERIMENTAL DATA. ALL VALUE ARE IN mT

θ	0°	30°	45°	60°	90°
M530-50A	61	79	56	93	46
M270-35A	133	164	134	72	45
M11535P	116	197	38	190	44
CGO35	74	148	27	128	26

V. CONCLUSION

In this paper an approach initially used to represent the IMR acquired by natural mineral assemblages and based on the use of the CDFs has been studied. An enhanced version, taking into account the anisotropic behavior of electrical steel, has been proposed and validated on two NO and two GO grades. It has been highlighted that the parameters defining the CDFs follow a 2nd order polynomial trendline. Based on this result, it has been shown that the model, taking into account both nonlinearity and anisotropy, can be fully derived from a number of experimental data limited to three only, which is a significant enhancement compared with other models dealt in the literature.

Furthermore, several sensibility analyses are to be done to improve the accuracy of the model. A first one would allow studying the impact of the curve fitting method used. A second one would allow determining the best set of three angles to consider to determine the polynomials. These are intended future activities.

ACKNOWLEDGMENT

The authors acknowledge the contribution of ThyssenKrupp Electrical Steel for providing both the NO and GO steel sheets. This work is co-financed by European Union with the financial support of European Regional Development Fund (ERDF), French State and the French Region of Hauts-de-France.

REFERENCES

[1] J.-P. Bastos and G. Quichaud, "3D modelling of a non-linear anisotropic lamination," *IEEE Trans. Magn.*, vol. 21, no. 6, pp. 2366–2369, Nov. 1985.

[2] J.-M. Dedulle, G. Meunier, A. Foggia, J.-C. Sabonnadiere, and D. Shen, "Magnetic fields in nonlinear anisotropic grain-oriented iron-sheet," *IEEE Trans. Magn.*, vol. 26, no. 2, pp. 524–527, Mar. 1990.

[3] J. Liu and G. Shirkoohi, "Anisotropic magnetic material modeling using finite element method," *IEEE Trans. Magn.*, vol. 29, no. 6, pp. 2458–2460, Nov. 1993.

[4] M. Enokizono and N. Soda, "Magnetic field analysis by finite element method using effective anisotropic field," *IEEE Trans. Magn.*, vol. 31, no. 3, pp. 1793–1796, May 1995.

[5] M. F. de Campos, "Anisotropy of steel sheets and consequence for Epstein test: I theory," in *XVIII IMEKO World Congress*, Rio de Janeiro, Brazil, Sep. 2006.

[6] K. Chwastek, A. P. S. Baghel, M. F. de Campos, S. Kulkarni, and J. Szczyglowski, "A Description for the Anisotropy of Magnetic Properties of Grain-Oriented Steels," *IEEE Trans. Magn.*, vol. 51, no. 12, pp. 1–5, Dec. 2015.

[7] H.-J. Bunge, "Texture and Magnetic Properties," *Textures Microstruct.*, vol. 11, no. 2-4, pp. 75–91, 1989.

[8] F. Jiang, M. Rossi, and G. Parent, "Anisotropy model for modern grain oriented electrical steel based on orientation distribution function," *AIP Advances*, vol. 8, no. 5, p. 056104, May 2018.

[9] D. Robertson and D. France, "Discrimination of remanence-carrying minerals in mixtures, using isothermal remanent magnetisation acquisition curves," *Phys. Earth Planet. Inter.*, vol. 82, no. 3-4, pp. 223–234, Mar. 1994.

[10] A. Paesano, T. J. B. Alves, R. F. Ferreira, R. Barco, M. I. Valerio-Cuadros, A. C. Viegas, D. Schafer, S. Nicolodi, and A. M. H. de Andrade, "Mathematical Analysis for the Hystereses of a Soft Ferromagnetic Steel by a Modified Rayleigh Model," *IEEE Trans. Magn.*, vol. 56, no. 4, pp. 1–7, Apr. 2020.

[11] Z. Sari and A. Ivanyi, "Statistical approach of hysteresis," *Phys. B: Condens. Matter*, vol. 372, no. 1-2, pp. 45–48, Feb. 2006.

[12] E. W. Ng and M. Geller, "A table of integrals of the error functions," *J. Res.Nat. Bureau of Standards B*, vol. 73, no. 1, pp. 1–20, Jan.–Mar. 1969.

[13] H. Stockhausen, "Some new aspects for the modelling of isothermal remanent magnetization acquisition curves by cumulative log Gaussian functions," *Geophys. Res. Lett.*, vol. 25, no. 12, pp. 2217–2220, Jun. 1998.

[14] R. Leonhardt, "Analyzing rock magnetic measurements: The RockMag-Analyzer 1.0 software," *Comput. and Geosci.*, vol. 32, no. 9, pp. 1420–1431, Nov. 2006.

[15] J. Sievert, H. Ahlers, M. Enokizono, S. Kauke, L. Rahf, and J. Xu, "The measurement of rotational power loss in electrical sheet steel using a vertical yoke system," *J. Magn. Magn. Mater.*, vol. 112, no. 1-3, pp. 91–94, Jul. 1992.

[16] W. Brix, K. Hempel, and W. Schroeder, "Method for the measurement of rotational power loss and related properties in electrical steel sheets," *IEEE Trans. Magn.*, vol. 18, no. 6, pp. 1469–1471, Nov. 1982.

[17] "IEC60404: Magnetic materials - Part 2: Methods of measurement of the magnetic properties of electrical steel strip by means of Epstein frame," 1992.